

# BASIC RESEARCH ON LIQUID-DROP-IMPACT EROSION

Quarterly Progress Report No. 2

For Period: December 8, 1966 Thru March 8, 1967

By

O. G. Engel

prepared for

NATIONAL AERONAUTICS AND SPACE ADMINISTRATION

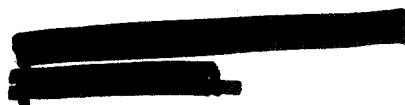
CONTRACT NASW-1481

SPACE POWER AND PROPULSION SECTION  
MISSILE AND SPACE DIVISION

**GENERAL  ELECTRIC**

CINCINNATI, OHIO 45215

IV 08 - 22292	(ACCESSION NUMBER)	32	(PAGES)	32	(CATEGORY)
	(THRU)				
FACILITY FORM 602					



### NOTICE

This report was prepared as an account of Government sponsored work. Neither the United States, nor the National Aeronautics and Space Administration (NASA), nor any person acting on behalf of NASA:

- A.) Makes any warranty or representation, expressed or implied, with respect to the accuracy, completeness, or usefulness of the information contained in this report, or that the use of any information, apparatus, method, or process disclosed in this report may not infringe privately owned rights; or
- B.) Assumes any liabilities with respect to the use of, or for damages resulting from the use of any information, apparatus, method or process disclosed in this report.

As used above, "person acting on behalf of NASA" includes any employee or contractor of NASA, or employee of such contractor, to the extent that such employee or contractor of NASA, or employee of such contractor prepares, disseminates, or provides access to, any information pursuant to his employment or contract with NASA, or his employment with such contractor.

Requests for copies of this report  
should be referred to:

National Aeronautics & Space Administration  
Scientific and Technical Information Division  
Attention: USS-A  
Washington, D.C. 20546

1136

BASIC RESEARCH ON LIQUID-DROP-IMPACT EROSION


QUARTERLY REPORT NO. 2

Covering the Period  
Dec. 8, 1966 to March 8, 1967

Written by  
Olive G. Engel

~~Prepared for~~  
NATIONAL AERONAUTICS AND SPACE ADMINISTRATION  
Contract NASW-1481

SPACE POWER AND PROPULSION SECTION  
MISSILE AND SPACE DIVISION  
GENERAL ELECTRIC COMPANY  
Cincinnati, Ohio 45215



# TABLE OF CONTENTS

Section	Page
1. Introduction . . . . .	1
2. Experimental Work . . . . .	1
2.1 Completion and Preliminary Test of the Gun . . . . .	1
2.2 Machining of Specimens . . . . .	4
2.3 State of the Metals Selected for Test . . . . .	5
2.4 Specimens of High-Purity Zinc . . . . .	6
2.5 Specimens of Armco Iron . . . . .	10
2.6 Specimens of Tantalum . . . . .	12
3. Theoretical Considerations . . . . .	14
3.1 Elastic Wave Theory Applied to the Impact of Rods . . . .	14
3.2 Application of One-Dimensional Elastic Wave Theory to Denting Velocity . . . . .	18
3.3 The Question of Dynamic Strength . . . . .	20
4. Work Plans for the Next Report Period . . . . .	20
5. References . . . . .	21

## LIST OF ILLUSTRATIONS

Figure	Page
1. Single Impact Apparatus Constructed at Battelle Memorial Institute (View 1) . . . . .	22
2. Single Impact Apparatus Constructed at Battelle Memorial Institute (View 2) . . . . .	23
3. X-Ray Diffraction Pattern of Zinc Impact Specimen Before and After Thermal Treatment . . . . .	24
4. X-Ray Diffraction Pattern of Zinc Impact Specimen Illustrating the Effectiveness of Grinding in Removing Surface Layer . . .	25
5. X-Ray Diffraction Pattern of Zinc Impact Specimen Illustrating the Effectiveness of Electropolishing in Removing Surface Distortion Left by 15- $\mu$ Diamond Grinding . . . . .	26
6. Impact of Two Rods . . . . .	15

## 1. Introduction

In accord with the work plans for this report period, construction and initial check-out of the gun at Battelle Memorial Institute has been completed. Impact specimens of zinc and Armco iron have been prepared and are ready for the room-temperature firings specified for the experiment; specimens of tantalum are in the final stage of preparation. Specimens for determination of the static tensile strength of these metals and specimens for determination of the speed of sound both in these metals and in the steel of which the steel spheres were fabricated are also essentially ready for use.

A review of one-dimensional elastic wave theory has been carried out in an effort to determine the physical significance of the factor of difference between eqs (2) and (5) of Quarterly Progress Report No. 1.

A detailed discussion of these topics is given below.

## 2. Experimental Work

The description of the single impact gun given in Quarterly Progress Report No. 1 was for the device as it was first conceived. A description of modifications which have been made in the gun, submitted by Mr. E.G. Bodine of Battelle Memorial Institute, follows.

### 2.1 Completion and Preliminary Test of the Gun

A single impact, helium-driven gas gun capable of accelerating  $3/32$ -inch- and  $5/32$ -inch-diameter steel spheres to velocities in excess of 1000 ft/sec has been designed and constructed. A unique feature of the gun is that it will allow specimens to be heated and tested in vacuum; this feature of the gun will minimize oxidation of the heated metal impact specimens. Since completion of the preliminary drawings, several modifications and improvements in the design of the gun have been made. The principal changes made were to (1) orient the gun vertically instead of horizontally and (2) redesign the furnace to allow alignment of the specimen in a more straight-forward manner than had been initially conceived. The reasons for making these changes follow.

Operation of the gun in a vertical line will eliminate the problem of correcting the position and tilt angle of the specimen impact face to account for the parabolic trajectory of the steel spheres. For example, in the horizontal configuration, the off-axis adjustment in the specimen required for the lower projectile velocities becomes equal to the radius of the projectile. See Table 1. In addition, the position of the photosensing devices must also be adjusted or their aperture must be opened to accommodate the expected variations in the projectile flight path. Since changes in the position of the photosensors is not desirable, the gun was constructed in the vertical configuration. The flight path at all velocities will now correspond to the true axis of the gun. Photographs of the apparatus with the furnace removed are shown in Figures 1 and 2.

---

Table 1

Vertical Correction from Optical Axis at Various Projectile Velocities for  
Horizontal Gun Axis

---

Velocity, $V_0$	$\sqrt{a}$ Time of Free Flight, $t$	$\sqrt{a}$ Vertical Correction, $S$
ft/sec	sec	inches
1000	0.003	0.0001
500	0.006	0.0006
200	0.015	0.0036
100	0.030	0.0145
50	0.060	0.0580

---

$\sqrt{a}$  For a free flight distance of 3.05 ft.

The second major modification involved changes in the furnace and in the specimen holder. In the preliminary gun design, the specimen holder was to be adjustable so that the specimen could be aligned with the axis of the gun while at temperature. After further consideration, it became obvious that a better scheme would involve moving the entire furnace rather than just the specimen holder. In this way, the necessity for making mechanical adjustments through the vacuum barrier could be avoided. The modified furnace arrangement as constructed provides freedom of motion in the horizontal plane as well as tilt adjustment to assure perpendicular impact. A metal bellows allows the necessary motion of the furnace without reducing the quality of the vacuum seal.

Although the modifications just described will result in an improvement in operation, they have caused an unavoidable delay in the final check-out of the gun. At present, the apparatus is in operation without the furnace. Room-temperature firings to check out components not associated with the furnace are being made and a number of small problems have been identified and corrected. For example, a change in the design of the sabot has been made to improve its projectile release characteristics on impact with the sabot catcher. In addition, the material of the sabot catcher has been changed from a high impact plastic to 6061-T6 aluminum alloy to reduce the variation in projectile velocity caused by accumulative deformation of the impacted surface. Photo-sensing devices with response times better than those of solid state photo-duo-diodes have been obtained (RCA 935 vacuum photo-diodes) and the necessary electronic circuitry for their operation has been constructed. The response time from the manufacturer's data sheets for the vacuum photo-diode is  $0.6 \times 10^{-9}$  seconds whereas for the solid state photo-duo-diode it is  $1.0 \times 10^{-6}$  seconds. The use of vacuum photo-diodes will reduce the uncertainty in velocity measurements essentially to the level of the uncertainty in the measurement of



position.

Two problems are still receiving attention. The first involves variations in projectile velocity. It is thought that these variations are associated with variations in operating time of the solenoid gas valve. This valve allows high pressure gas to enter the gun breech and small variations in its operating time will result in variation in the projectile velocity. A more reproducible electric valve is being sought. Plans for a fast-acting piston valve of the type used in hypervelocity light-gas guns have been requested from Air Force Special Weapons Center. In addition, a precision rupture disk valve has been ordered with a wide range of associated rupture disks. Further tests will be made to isolate the causes of projectile velocity variations and an appropriate valve system will then be selected.

The second problem still receiving attention has to do with the optical alignment of the specimen. On receiving the electropolished zinc specimens, it became obvious that the impact face of these specimens could not be counted upon to reflect enough light for the collimation scheme which was to be employed. An alternate scheme, which involves a thin quartz first-surface mirror, is being considered. It has the disadvantage that a test firing could not be performed without first removing the quartz alignment mirror. Alignment at temperature would be impractical in this situation. Other alternatives, such as alignment from the rear surface, will be explored.

## 2.2 Machining of Specimens

Twenty specimens for steel-sphere firings, two tensile specimens for determination of static yield strength, and one specimen for determination of infinite medium sound speed were machined from each of the three metals that have been received to date for use in the experiment. These metals are

zinc, Armco iron, and tantalum. In addition, a specimen to be used for determination of infinite medium sound speed was machined from an end of round bar stock of AISI 52100 chrome alloy steel which has the same composition as that of the steel spheres to be used in the firings.

### 2.3 State of the Metals Selected for Test

At the suggestion of Dr. J.W.Semmel, Jr., manager of SPPS Materials and Processes, and of Dr. Cecil G. Dunn of General Electric Research Laboratory, Schenectady, N.Y., the criterion adopted for annealing conditions to be used for the metals was a compromise between two requirements. These requirements are that the maximum amount of cold work should be removed from the metals and that the grain size should be maintained as small as possible.

The first requirement is dictated by the need to test the metal in its most characteristic strength state. This requirement can be fulfilled satisfactorily by recrystallization alone. Most of the work in a metal is removed by recrystallization; after recrystallization is complete there is essentially only an increase in grain size.

The second requirement is dictated by the fact that, if the grain size is large in comparison with the size of the impinging spheres, scatter may be introduced into the crater-depth data. Scatter is to be expected if the grain size is large in comparison with the sphere size because target areas covered by some impacts may lie wholly within single grains whereas those covered by other impacts may extend across one or more grain boundaries.

Because grain size starts to increase as soon as recrystallization is complete, the desired annealing conditions are those that will produce maximum recrystallization with minimum grain growth. Preliminary studies, which were carried out to determine the optimum processing conditions for the

specimens of each of the three metals that have been received for use in the experiment are described below.

## 2.4 Specimens of High-Purity Zinc

### Composition and Processing History of the Metal

The metal, which was purchased from Calrex Corporation at Campbell, O., consisted of round rod having a diameter of 1.25 inch. The metal supplied was from one heat. The purity of this metal, as reported by Mr. John Stavich, is high; it is 99.997 percent zinc. The major impurities are: lead, 0.001 per cent; cadmium, 0.0005 per cent; and iron, 0.0015 per cent.

The metal was cast and then extruded as rod.

### State of the Metal in a Machined Specimen

Impact test specimens cut from this rod were right circular cylinders having diameter  $1.000 \pm 0.016$  inch and length  $0.500 \pm 0.016$  inch. The impact face of the specimens was ground to a 15 rms microinch finish in the machine shop. A study was carried out by Mr. L.B.Engel of SPPS Physical Metallurgy and Mr. H.J.Bauer of SPPS Metallography to determine the state of the metal from the surface inward.

An X-ray diffraction pattern was obtained of the as-ground surface of one specimen selected for the study. Layers 0.003 and 0.025 inch in thickness were then successively removed with use of dilute hydrochloric acid. An X-ray diffraction pattern of the newly exposed surface was obtained after each layer removal using sufficiently large values of the diffraction angle,  $2\theta$ , to insure detection of any line broadening or line shift. The results are given in Table 2.

Comparison of the data in Table 2 for the as-ground surface with the ASTM powder data for zinc shows that the d-spacings are in good agreement and all of the reflections are present. The differences in relative intensities

Table 2. X-ray Diffraction Data for Zinc Impact Specimens

	ASTM Data		As-Ground		0.003 in. Removed with Dilute HCl		0.028 in. Removed with Dilute HCl		0.028 in. Removed and 1 Hour at 350° F	
	d(Å)	I/I <sub>1</sub>	d(Å)	I/I <sub>1</sub>	d(Å)	I/I <sub>1</sub>	d(Å)	I/I <sub>1</sub>	d(Å)	I/I <sub>1</sub>
hk·l										
10·5	0.909	55	0.909	5	✓		0.909	9	✓	
11·4	0.906	100	0.906	55	✓		✓		✓	
21·0	0.872	45	0.872	15	0.872	100	0.872	100	0.872	100
21·1	0.859	82	0.859	100	0.858	31	0.859	24	✓	
20·4	0.844	18	0.843	5	✓		✓		✓	
00·6	0.825	9	0.824	30	✓		0.824	12	✓	
21·2	0.823	82	0.822	17	0.822	9	0.823	19	✓	

a/ Obtained with General Electric XRD-3 Diffractometer using Cu-K<sub>α</sub> radiation (48 KV, 16 Ma).

b/ Data reported on ASTM X-ray powder file card number 4-0831.

c/ Relative intensities calculated relative to most intense line observed between 0.909  $\geq$  d  $\geq$  0.822.

d/ No reflection detected.

indicate a preferred orientation in the surface layer. Metallographic examination revealed equiaxed grains of size approximately equivalent to ASTM No. 6; the equiaxed character of the grains suggests that the metal in the surface layer recrystallized as a result of heating during the surface grinding operation.

For the surface exposed after removal of a 0.003-inch layer of metal, non-uniform intensities and missing reflections in the data of Table 2 indicate a preferred orientation and possibly a large grain size. Metallographic examination revealed equiaxed grains of size approximately equivalent to ASTM No. 2; the equiaxed character of these grains in conjunction with their large size suggests that this metal annealed at a temperature in excess of its recrystallization temperature at the time that the zinc rod was extruded. The d-spacings of the observed reflections are again in good agreement with the ASTM powder data for zinc.

Because the data of Table 2 for the surfaces that were exposed after removal of a 0.003-inch layer of metal and after removal of an additional 0.025-inch layer of metal are similar, it was concluded that a preferred orientation does exist in the zinc rod and that the depth of the surface layer of recrystallized metal was less than 0.003 inch on this specimen. The depth of the surface layer of recrystallized metal can be expected to vary from specimen to specimen depending on the extent of surface grinding received.

The effect that thermal treatment might have was investigated by heat treating the specimen after the surface metal had been removed to a total depth of 0.028 inch. The specimen was heated at 350°F for one hour and an X-ray diffraction pattern was then obtained. Because there is no line shift (see Table 2), which is indicative of uniform strain, and no significant changes in line width (see Figure 3), which are indicative of non-uniform strain, it was

concluded that holding the specimen at 350°F for one hour had essentially no effect on it.

It was decided to remove the surface layer of recrystallized metal from the remaining zinc specimens that had been prepared for use as targets in the steel-sphere-impact experiment. The 0.003-inch and 0.025-inch layers of metal had been removed from the specimen selected for preliminary study with use of dilute hydrochloric acid. This method of removal could have been used to remove the layer of recrystallized metal from the remaining specimens. However, the acid treatment appeared to pit the surface and surface pits were considered to be objectionable in specimens to be used in an impact study. The effect of a combination of metallographic grinding and electropolishing on removing the small-grained surface layer was, therefore, evaluated.

Because the (11·4) reflection observed in the as-ground surface was found to disappear upon removal of the surface layer, the intensity of this reflection was used as an indicator to assess the effectiveness of grinding and electropolishing on removing the surface layer. The minimum amount of distortion that resulted from various grinding techniques was determined and the following grinding procedure was adopted. Step 1, remove from 0.005 to 0.010 inch from the specimen on a water-cooled, 380-rpm, 600-grit (silicon carbide) wheel; Step 2, grind for one hour on a 55-rpm wheel covered with nylon cloth containing 15- $\mu$  diamond paste and using a 200-gram load.

The effectiveness of each step in removing the surface layer is shown in Figure 4. Although the grinding with 15- $\mu$  diamond (Step 2) appears to have removed the surface layer as evidenced by the disappearance of the (11·4) reflection, some surface distortion was indicated by line broadening and an intensity shift in the (21·0) reflection. This distortion is considered to

be the residual effect of the grinding with 15- $\mu$  diamond. It was removed by electropolishing in an air-agitated, 20 per cent aqueous potassium hydroxide solution for ten minutes at a current density of 16 amp/dm<sup>2</sup> at room temperature using a copper cathode. See Figure 5.

The final surface finish was considered adequate and the remaining twenty zinc impact specimens were prepared with use of the technique described. These specimens have been forwarded to Mr. E.G. Bodine at Battelle Memorial Institute for use in the firings.

The tensile specimens of zinc are in process of being finished in a similar way. It was considered preferable not to electropolish the contact surfaces of the specimen made for determination of infinite medium sound speed.

## 2.5 Specimens of Armco Iron

### Composition and Processing History of the Metal

The metal, which was purchased from Lapham Hickey Steel at Chicago, Ill., was cold drawn Armco magnetic ingot iron. The metal was from one heat (No. 66080) and was supplied as one round rod having diameter 1.0000  $\pm$  0.0075 inch.

The certified test report submitted by the vendor indicates that the following elements could be present in the specified amounts: carbon, 0.025 per cent; manganese, 0.054 per cent; phosphorus, 0.006 per cent; sulfur, 0.011 per cent; silicon, trace; and copper, 0.062 per cent. Presuming that the balance is iron, the iron content is 99.842 per cent.

For a further check on the purity of this metal, it was subjected to N S L spectroscopic survey. The major impurities were found to be: copper, 0.049 per cent; manganese, 0.003 per cent; cobalt, less than 0.005 per cent. The following elements were found in less than 0.001 per cent: silver, aluminum, magnesium, nickel, chromium, vanadium, silicon, zirconium, sodium, tin,

potassium, lithium, and molybdenum. The following elements were looked for and not detected: arsenic, boron, bismuth, calcium, columbium, cadmium, lead, antimony, strontium, barium, titanium, tungsten, and zinc. Carbon was determined separately by Mr. Harold Bradley of SPPS Chemistry and Physics using high temperature combustion followed by a conductimetric determination of carbon dioxide. Results obtained for two specimens of the metal were 80 and 85 ppm, respectively.

On the basis of the separate determination of carbon and of the spectroscopic results for manganese, cobalt and copper in conjunction with the certified test results for phosphorus and sulfur, the iron content is 99.918 per cent presuming that the balance is iron.

The reported processing history of the rod was as follows: hot and cold worked to a diameter of 1.25 inch; annealed; cold drawn to a diameter of 1 inch. Data on the as-received condition of the metal are as follows: structure, cold worked; grain size, approximately ASTM No. 5 to No. 6.

#### Polishing

Impact test specimens cut from the iron rod were right circular cylinders having diameter  $1.000 \pm 0.016$  inch and length  $0.500 \pm 0.016$  inch. The impact face of the specimens was ground to a 15 rms microinch finish in the machine shop.

The impact face of each specimen to be used in the test firings was then given a high polish by Mr. H.J.Bauer of SPPS Metallography. The polishing procedure, carried out on a Struers mover and variable-speed wheel using a 500-gram load at 100 rpm, was as follows: Step 1, four hours on nylon cloth with 45- $\mu$  diamond paste; Step 2, three hours on nylon cloth with 6- $\mu$  diamond paste; Step 3, four hours on polytech Pre-PS cloth with 0.1- $\mu$  diamond



paste.

### Heat Treatment

A study to determine the temperature and time required to produce maximum recrystallization with minimum grain growth in this metal was carried out by Mr. W.F. Zimmerman, manager of SPPS Ceramic Materials, in conjunction with Mr. D.S. Engleby. It was found that heating at temperatures from 1100 to 1550°F for one hour reduced the hardness of the metal but left it with a fibrous structure. Recrystallization to a fine-grained structure was obtained when a specimen of the metal was heated for three hours at 1750°F, which is above the alpha-to-gamma transformation temperature.

All of the iron specimens (the polished impact specimens, two tensile specimens, and a specimen for determination of infinite medium sound speed) were then heat treated in a Brew-type laboratory furnace at 1750°F in a vacuum of  $6 \times 10^{-6}$  mm mercury for three hours and furnace cooled. The grain size of the heat treated specimens, as determined by micro-examination at a magnification of 100.X, was a uniform ASTM No. 4 to No. 5. The hardness of the heat treated specimens was found to be Brinell 70 (equivalent) which is lower than the reported  $\sqrt{1}$  hardness of fully annealed ingot iron.

### 2.6 Specimens of Tantalum

#### Composition and Processing History of the Metal

The metal, which was purchased from Union Carbide Corporation at Kokomo, Ind., was Haynes tantalum of ASTM specification B-365-62T. The metal was from one heat (No. 81444) and was supplied as one piece of round rod having a diameter of  $1.0000 \pm 0.0075$  inch.

The certified report of chemical analysis lists the following elements in the amounts specified: tungsten, less than 0.01 per cent; iron, less than 0.01 per cent; carbon, 0.001 per cent; silicon, less than 0.01 per cent;

nickel, less than 0.005 per cent; columbium, 0.10 per cent; titanium, less than 0.01 per cent; oxygen, 0.0077 per cent; hydrogen, 0.0003 per cent; nitrogen, 0.0012 per cent; balance tantalum. On the basis of this analysis, the metal supplied is at least 99.845 per cent tantalum.

The reported processing history is a 96 per cent reduction in area. The as-received condition of the metal was as follows: structure, cold worked; hardness, 81.2 DPH.

#### Polishing

Impact test specimens cut from the tantalum rod were right circular cylinders having diameter  $1.000 \pm 0.016$  inch and length  $0.500 \pm 0.016$  inch. The impact face of the specimens was ground to a 15 rms microinch finish in the machine shop.

The impact face of each specimen to be used in the test firings was given a metallographic polish by Mr. H.J.Bauer of SPPS Metallography. The polishing procedure, carried out on a Struers mover and variable-speed wheel using a 500-gram load at 100 rpm, was as follows: Step 1, four hours on nylon cloth with  $45\text{-}\mu$  diamond paste; Step 2, twenty minutes on polytech Supreme cloth with  $0.05\text{-}\mu$  alumina in 30 per cent hydrogen peroxide.

#### Heat Treatment

A study to determine the temperature and time required to produce maximum recrystallization with minimum grain growth in this metal has been initiated by Mr. W.F.Zimmerman, manager of SPPS Ceramic Materials, in conjunction with Mr. D.S.Engleby. Furnace cooling after heat treatment in a Brew-type laboratory furnace at  $2100^{\circ}\text{F}$  and in a vacuum of  $6 \times 10^{-6}$  mm mercury for one hour has been found to produce 90 to 95 per cent recrystallization with a grain size of ASTM No. 3 to No. 5 and a hardness of 49 DPH. Further study of the heat treatment of this metal is in progress to improve the extent of recrystallization.

### 3. Theoretical Considerations

In Quarterly Progress Report No. 1, it was pointed out that the equation for denting velocity that best describes the experimental data can be written in the form

$$V_i = 19 (zc/z'c')^{\frac{1}{2}} \left[ E' (z + z') / z z' \right]. \quad (1)$$

Here  $E'$  is taken to be the dynamic compressive yield strength of the target material,  $c$  is the velocity of sound in infinite medium, and  $z$  is acoustic impedance ( $z = c\rho$  where  $\rho$  is density).

It was further pointed out that on the basis of one-dimensional elastic-wave theory, it was thought that denting velocity should be given by

$$V_i = k \left[ E' (z + z') / z z' \right] \quad (2)$$

where  $k$  is a numerical constant. The factor of difference between eqs (1) and (2) is  $(zc / z'c')^{\frac{1}{2}}$ . In a search for the physical significance of this factor, the fundamental concepts of one-dimensional elastic-wave theory relating to the simple case of the impact of two solid rods with flat ends was reviewed.

#### 3.1 Elastic Wave Theory Applied to the Impact of Rods

A fairly general case of the impact of rods is that two rods of different materials, each having a velocity of its own, approach and collide.

##### Interface Boundary Conditions

Let rods  $R$  and  $R'$ , composed of materials  $M$  and  $M'$  and moving at velocities  $V$  and  $V'$ , respectively, where  $V - V' > 0$ , approach and collide. As soon as collision occurs, waves of compression, which originate at the impact interface, begin to move through each of the rods<sup>2</sup>. If a very short time interval,  $\Delta t$ , associated with the instant of impact is

considered, the amounts of material of each rod that are traversed by the respective compressional waves are extremely small and it can be assumed that in this short time there is no gain or loss of momentum.

The distances that the compressional waves, which originate at the impact interface, move into the rods in the short time  $\Delta t$  are  $c \Delta t$  and  $c' \Delta t$ , respectively. The situation is shown diagrammatically in Figure 6 for the case that  $c > c'$ ,  $V > V'$ , and rods R and R' are moving along the x-axis.

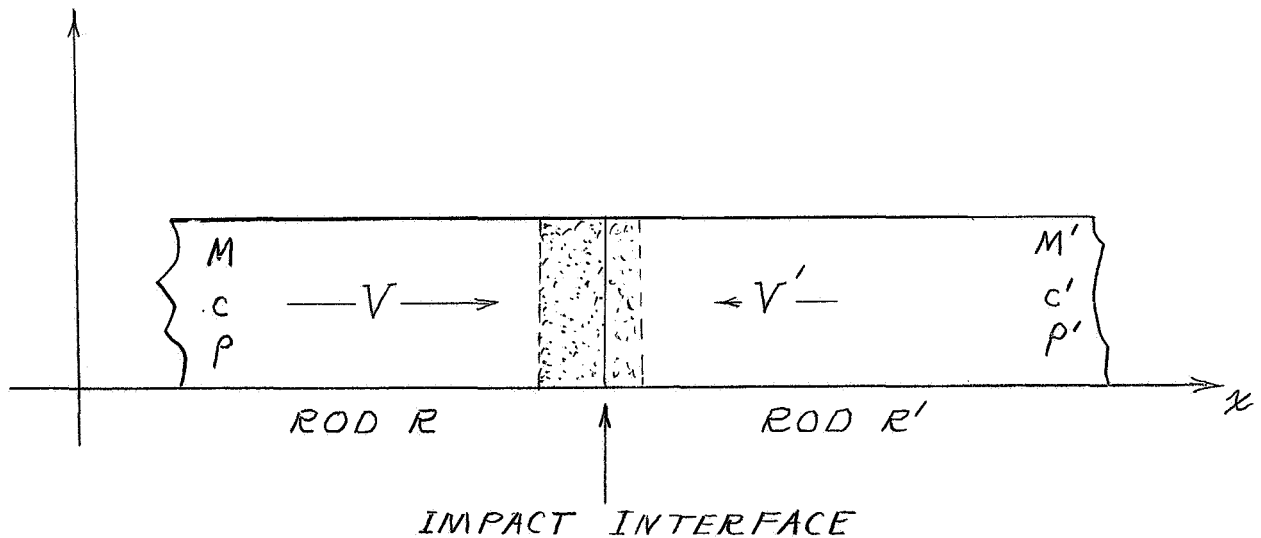


Figure 6. Impact of Two Rods

Two boundary conditions must be met at the impact interface. First, in order that the bars simply remain in contact without one bar penetrating the other or one bar receding from the other, the material traversed by the compressional waves initiated in each rod must have the same velocity (a common velocity). Secondly, the compressive force in the material of each rod traversed by the respective compressional waves must be equal because the equation for one-dimensional longitudinal elastic-wave motion is based on a

balance of force across an element of a rod. The result of the second boundary condition is that there is no pressure difference across the impact interface.

### Velocities

Let the common velocity, required by the first boundary condition, be  $V$ . To simplify the mathematical equations, let the rods each be cylindrical and of unit cross-sectional area. Conservation of momentum during the short time,  $\Delta t$ , requires that

$$c \Delta t \rho V + c' \Delta t \rho' V' = c \Delta t \rho V + c' \Delta t \rho' V. \quad (3)$$

Dividing eq (3) by  $\Delta t$  and solving for the common velocity  $V$  produces

$$\begin{aligned} V &= (c \rho V + c' \rho' V') / (c \rho + c' \rho') \\ &= (z V + z' V') / (z + z'). \end{aligned} \quad (4)$$

The common velocity given by eq (4) is equivalent to that found by Saint-Venant<sup>2</sup> who increased the generality of the case by considering rods with different cross-sectional areas.

The case in which one of the rods is at rest at the time that impact occurs is less general. If rod  $R'$  is chosen to be the rod at rest, then from conservation of momentum,

$$c \Delta t \rho V = c \Delta t \rho V + c' \Delta t \rho' V \quad (5)$$

and

$$V = c \rho V / (c \rho + c' \rho') = z V / (z + z'). \quad (6)$$

Knowing the common velocity  $V$ , the particle velocities in the compressed zones,  $v$  and  $v'$ , which are lost by rod  $R$  and gained by rod  $R'$ , respectively, as a result of the impact, can be determined.

$$V - v = \mathcal{V} = (zV + z'V') / (z + z')$$

$$v = z' (V - V') / (z + z') \quad (7)$$

Similarly,

$$V' + v' = \mathcal{V} = (zV + z'V') / (z + z')$$

$$v' = z (V - V') / (z + z') \quad (8)$$

For the less general case, in which rod  $R'$  is at rest when the impact occurs,

$$v' = \mathcal{V} = z V / (z + z') \quad (9)$$

and  $V - v = \mathcal{V} = z V / (z + z')$

$$v = z' V / (z + z') \quad (10)$$

### Stresses

With the rods aligned along the x-axis as in Figure 6, unit shortenings  $\partial u / \partial x$  and  $\partial u' / \partial x$  are associated with the total shortenings,  $u$  and  $u'$ , due to compression in the two rods, respectively. According to the second boundary condition imposed, the compressive force in the compressed section of rod  $R$  is equal to the compressive force in the compressed section of rod  $R'$ . Because the compressive force is given by the product of the cross-sectional area,  $A$ , Young's modulus,  $Y$ , and the unit elongation<sup>3</sup>, it follows that

$$A Y (\partial u / \partial x) = A' Y' (\partial u' / \partial x). \quad (11)$$

Because the unit shortening,  $\partial u / \partial x$ , is given by<sup>4</sup>

$$\partial u / \partial x = v/c, \quad (12)$$

and because for a rod,

$$Y = c^2 \rho = c z \quad (13)$$

the compressive force per unit area, or compressive pressure  $\sigma$ , in the compressed zone of rod R is  $(c^2 \rho / c) [z' (V - V') / (z + z')]$ , and, with use of eq (9),

$$\sigma = z z' (V - V') / (z + z') = z' z (V - V') / (z + z') = \sigma'. \quad (14)$$

For the less general case, in which rod R' is at rest when the impact occurs,

$$\sigma = z z' V / (z + z') = z' z V / (z + z') = \sigma'. \quad (15)$$

### 3.2 Application of One-Dimensional Elastic-Wave Theory to Denting Velocity

The intercept velocity,  $V_i$ , is the velocity below which no dent is produced in a solid target as a result of being struck by another mass (liquid or solid). It is the threshold velocity for which the strain energy in the elastic wave generated in the solid target material is equal to but does not exceed the energy per unit volume that the target solid can accept without plastic flow.

The strain energy of deformation in the elastic wave is given by  $\sqrt[3]{}$  the quotient  $\sigma'^2 / 2 Y'$ . The strain energy in the solid at the yield stress is  $\sigma'_y \epsilon'_y / 2$ , where sub-y refers to the yield point. Using eq (15) for  $\sigma'$  and the condition for the threshold velocity given above,

$$\left[ z z' V_i / (z + z') \right]^2 (1 / 2 Y') = \sigma'_y \epsilon'_y / 2. \quad (16)$$

Multiplying eq (16) by 2 and substituting eq (12) for the unit shortening,

$\epsilon'_y$ , produces the expression

$$\left[ z z' V_i / (z + z') \right]^2 (1/Y') = \sigma'_y (v' / c') . \quad (17)$$

For the threshold condition, the particle velocity,  $v'$ , is given by eq (9) with  $V = V_i$ . Dividing both sides of eq (17) by this particle velocity, and multiplying both sides by  $c'$ , produces the equality

$$\left[ z z' V_i / (z + z') \right] (z' c' / Y') = \sigma'_y . \quad (18)$$

If the explicit expression for  $Y'$ , given by eq (13), is substituted into eq (18), this equation reduces to

$$z z' V_i / (z + z') = \sigma'_y \quad (19)$$

from which

$$V_i = \sigma'_y (z + z') / z z' . \quad (20)$$

With  $\sigma'_y$  set equal to  $E'$ , which was taken to be the dynamic compressive yield strength, eq (20) is identical with eq (2).

The review of the fundamental concepts of one-dimensional elastic-wave theory has thrown no light on the physical significance of the factor  $(z c / z' c')^{\frac{1}{2}}$  which is required by the empirical equation for the denting velocity, eq (1). It is possible that at the yield point of the material of either of two rods that collide, the second boundary condition for a purely elastic impact (equal compressive forces) may break down. If time permits, further consideration will be given to this question during the next report period.



### 3.3 The Question of Dynamic Strength

It was pointed out in Quarterly Progress Report No. 1 that the concept of dynamic strength of metals (strain rate effects) has been called into question for pure metals and simple alloys. During this report period this question has been discussed with Dr. Thad Vreeland of the California Institute of Technology, Pasadena, Calif., Dr. George Irwin, of the Naval Research Laboratory, Washington, D.C., and with Dr. N.J. Huffington, Jr., Chief of Dynamics Research, Martin Co., Baltimore, Md. Study of this question is still in progress.

### 4. Work Plans for the Next Report Period

Room-temperature firings against the zinc specimens are being initiated at the present time at Battelle Memorial Institute. The specimens of Armco iron are ready to be sent for use in the firings and it is hoped that the tantalum specimens will be ready in not more than two weeks. It is expected that all room-temperature firings on zinc, Armco iron, and tantalum will be completed during the next report period. It is also expected that the determination of tensile strength and the measurement of infinite medium sound speed for these metals will be made during the next report period.

Delivery of Udimet 700 for use in the steel-sphere impact experiment was expected by January 10, 1967. This metal has not yet been delivered; a revised estimate of the delivery date is now that the metal will be shipped by March 31, 1967. Nickel 270 for use in the experiment was to be available by April 1, 1967, and notice has been received that this date is still firm. It is hoped that specimens of these metals will be machined and ready for use in firings both at room temperature and at elevated temperatures before the end of the next report period.

## 5. References

1. Metals Handbook, 8th Edition, American Society for Metals, Nonety, O.,  
page 1211 of Vol. I.
2. B. d. Saint-Venant, Journal of Mathematics Pure and Applied, 2nd Series,  
Vol. 12 (1867).
3. S. Timoshenko and J.N.Goodier, Theory of Elasticity, 2nd Edition, McGraw-  
Hill Book Co., Inc., 1951.
4. A.E.H.Love, Mathematical Theory of Elasticity, 4th Edition, Dover Publica-  
tions, New York, N.Y., 1944

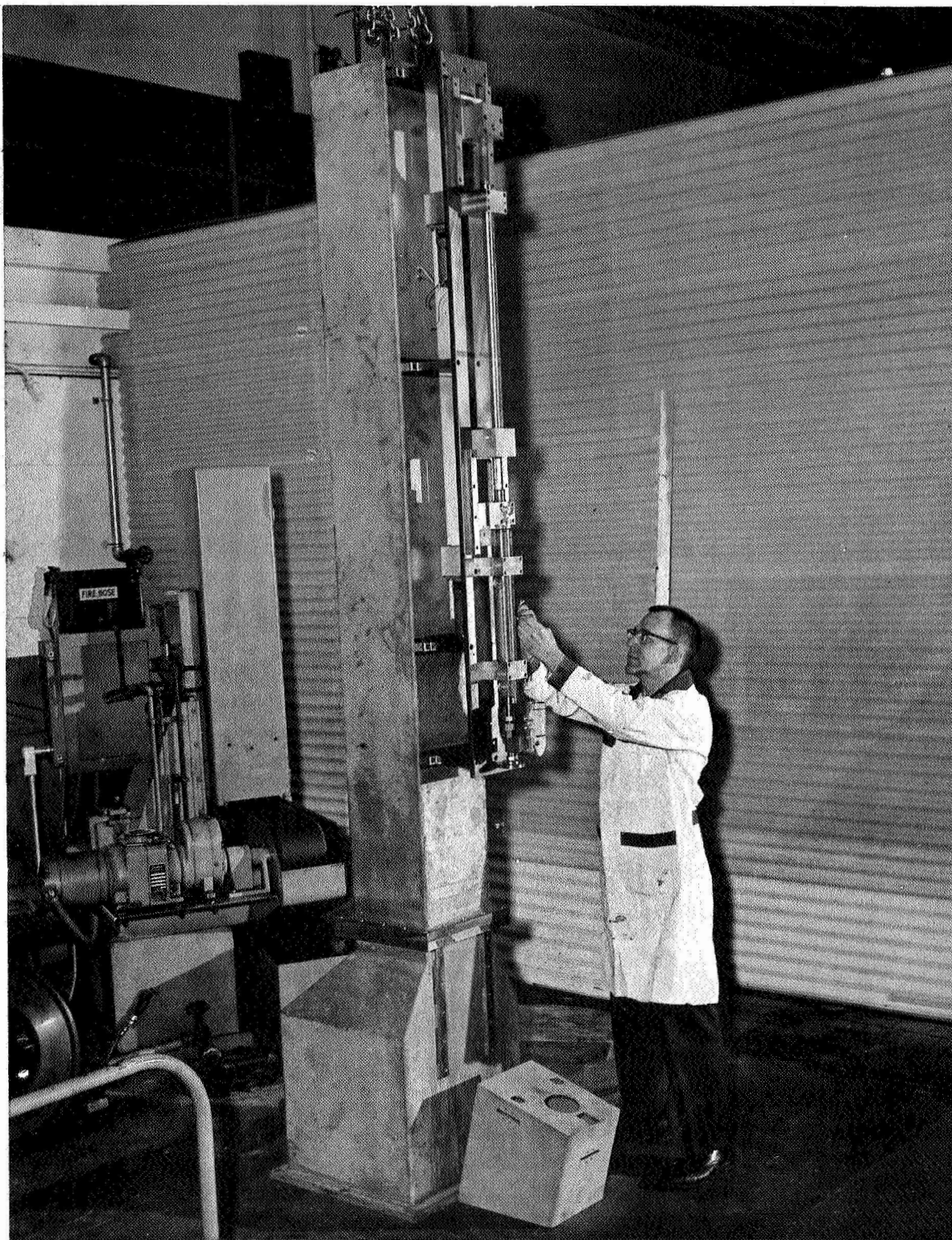


Figure 1. Single Impact Apparatus Constructed at Battelle Memorial Institute. View 1

R1197-1

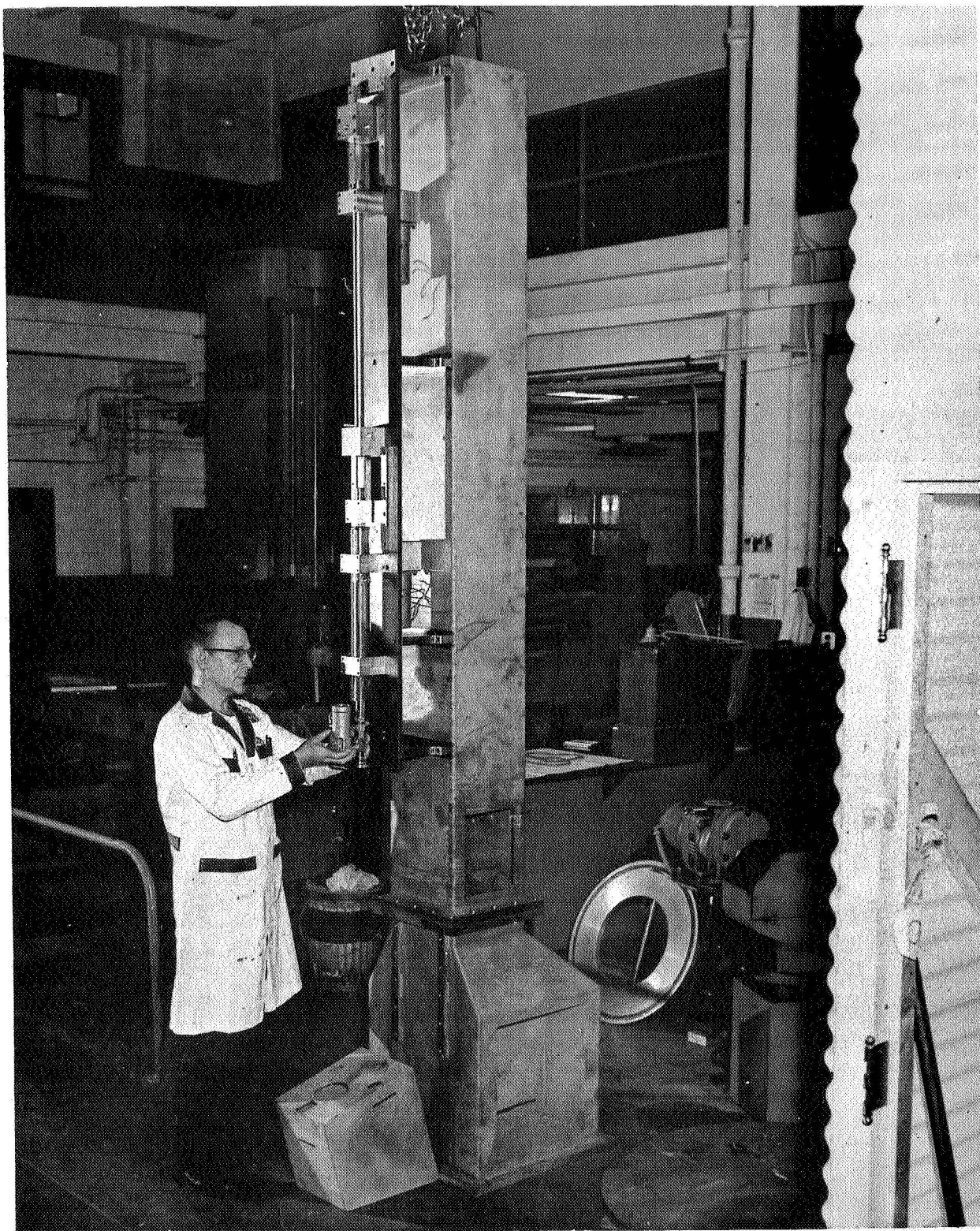


Figure 2. Single impact Apparatus Constructed at Battelle Memorial Institute. View 2

R1197-2

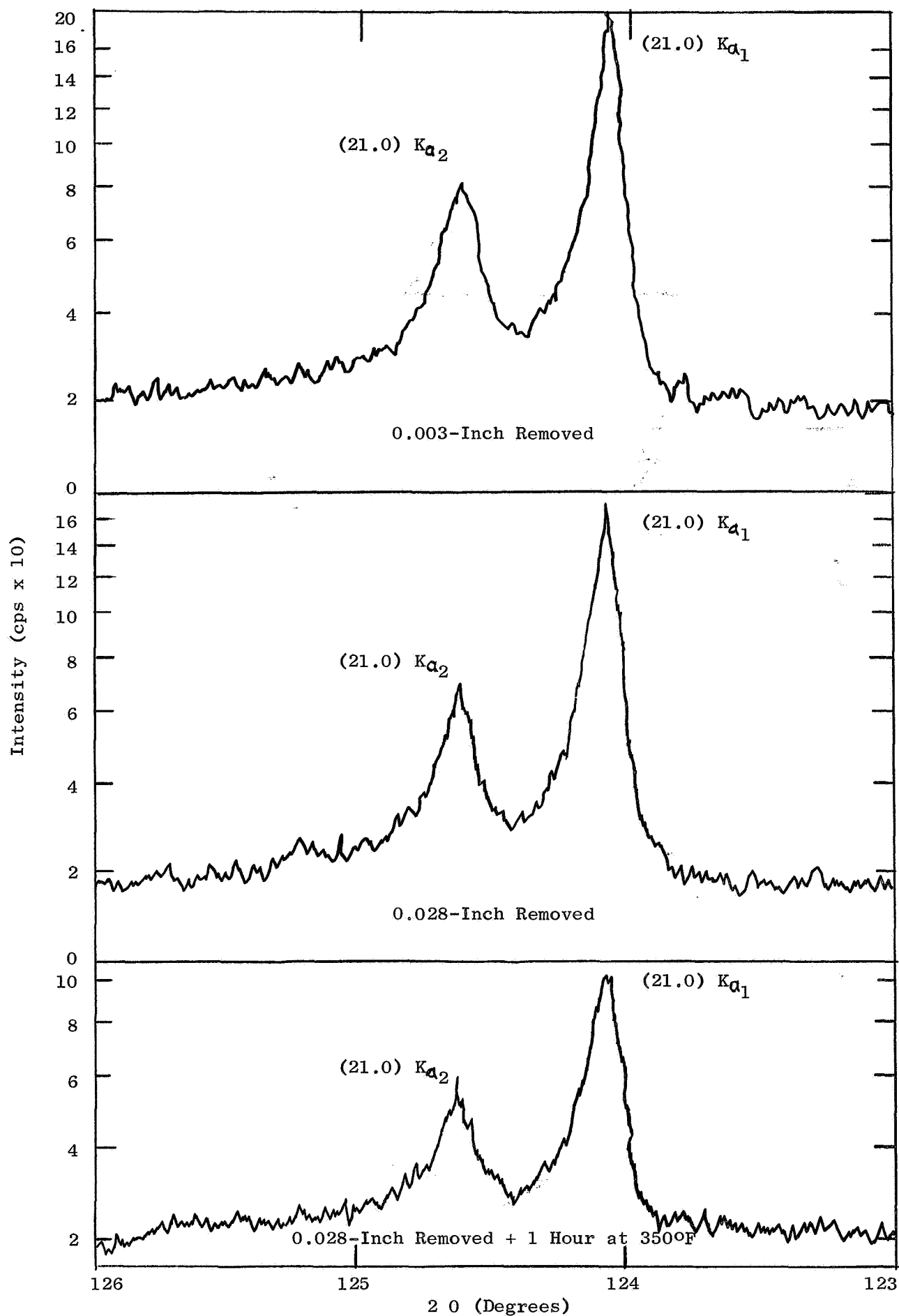


Figure 3. X-ray Diffraction Pattern of Zinc Impact Specimen Before and After Thermal Treatment.

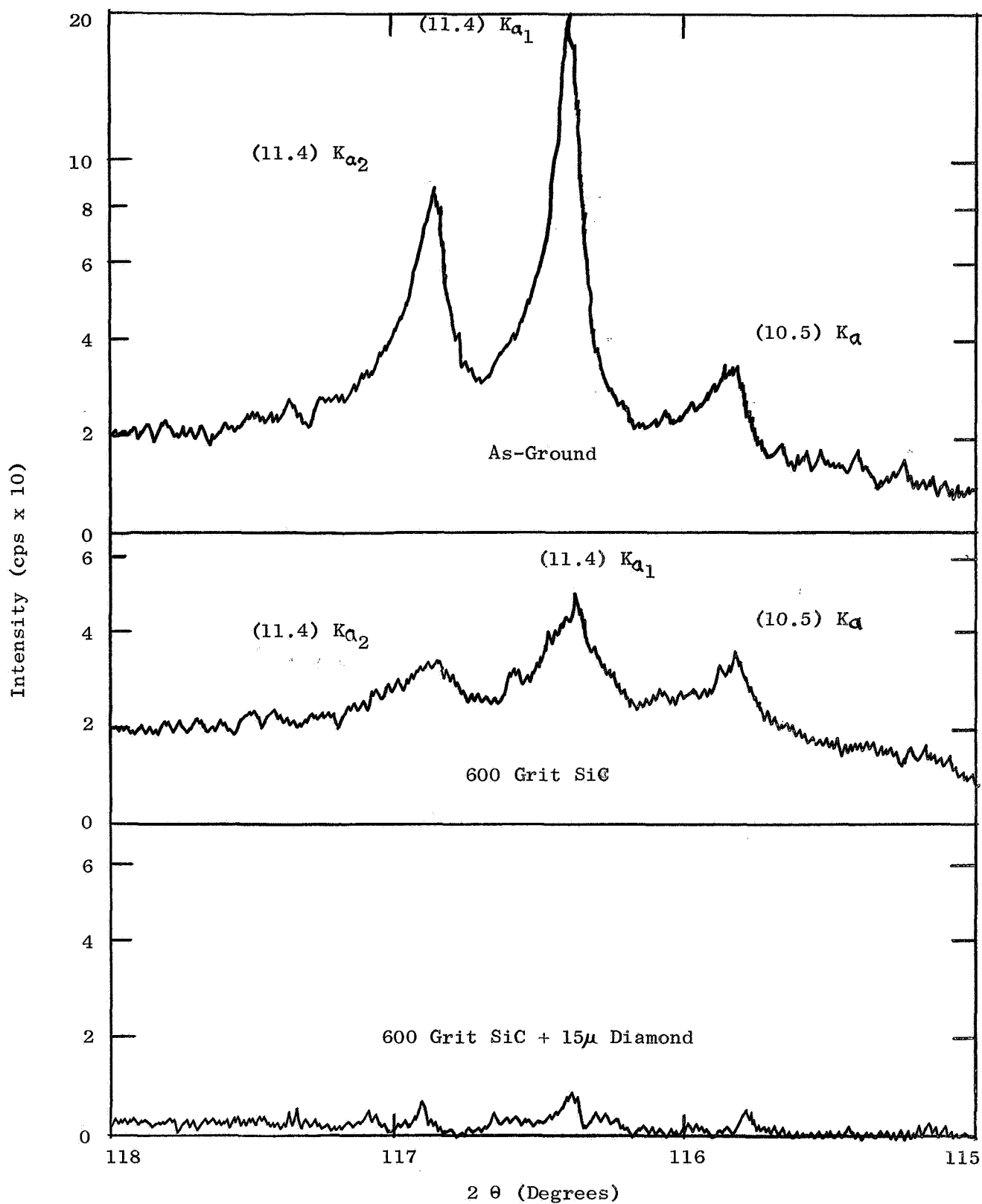


Figure 4. X-ray Diffraction Pattern of Zinc Impact Specimen Illustrating the Effectiveness of Grinding in Removing Surface Layer.

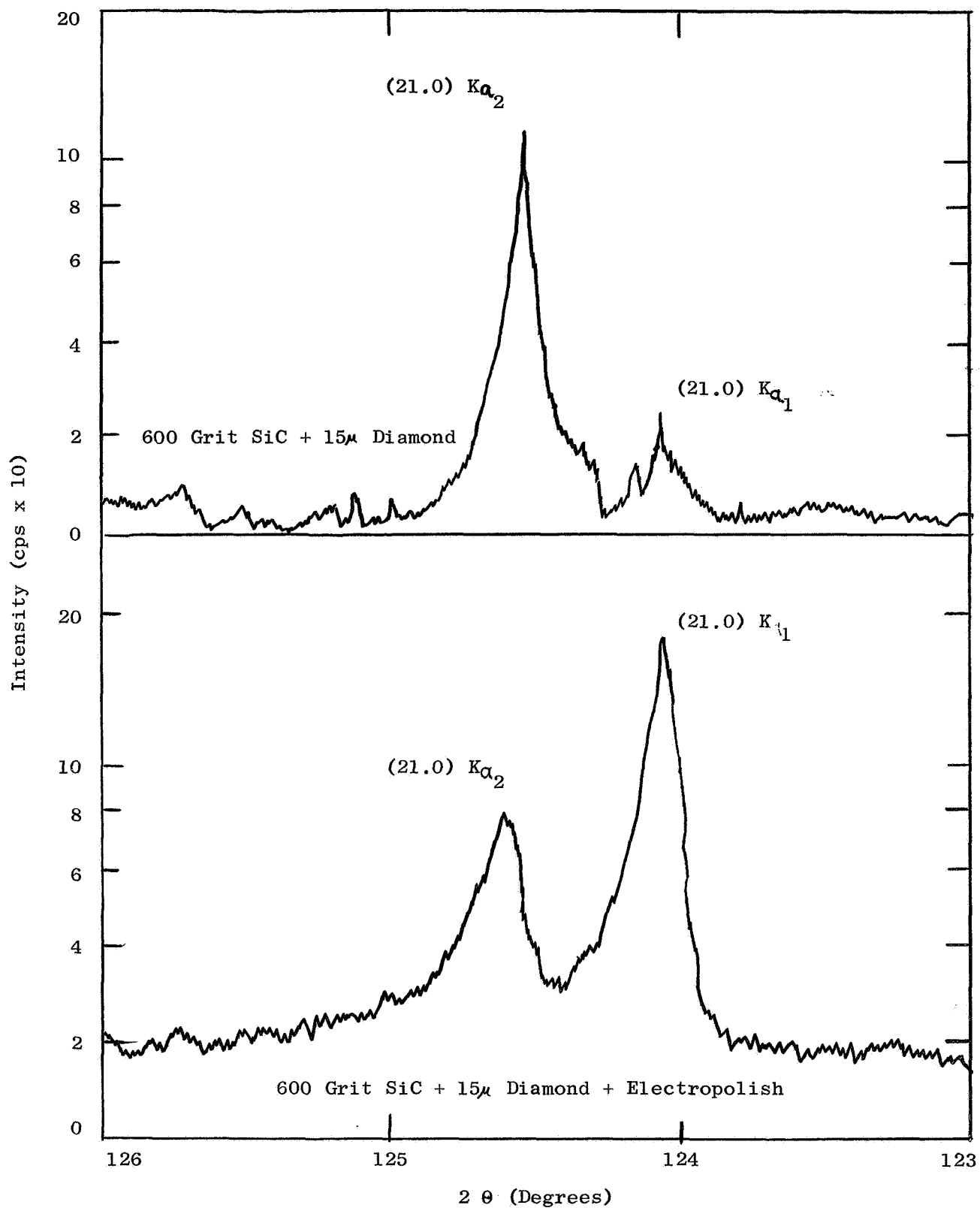


Figure 5. X-ray Diffraction Pattern of Zinc Impact Specimen Illustrating the Effectiveness of Electropolishing in Removing Surface Distortion Left by 15μ Diamond Grinding.